

# Comparison of Xilinx Virtex-II FPGA SEE Sensitivities to Protons and Heavy Ions

R. Koga, J. George, G. Swift, C. Yui, L. Edmonds, C. Carmichael, T. Langley, P. Murray, K. Lanes, and M. Napier

**Abstract**—A comparison of heavy-ion and proton-induced single event effect sensitivities has been made using the Xilinx Virtex-II field programmable gate array (FPGA). Recently fabricated test samples are selected for observations of single event upset and single event functional interrupt. A complex relationship appears to exist between the heavy ion and proton sensitivities due to effects such as multiple-bit upsets and elastic nuclear scattering.

**Index Terms**—Field programmable gate array (FPGA), heavy ion radiation effects, proton radiation effects, semiconductor device testing, single event effects.

## I. INTRODUCTION

THE Xilinx Virtex-II field programmable gate array (FPGA) is a useful microcircuit implementing reconfigurable computing (RCC). It is a static random access memory (SRAM) configured, high gate- and pin-count device of present interest to many designers. However, it is sensitive to single event effects (SEE) caused both by heavy ions [1] and protons. Excluding extremely sensitive microcircuits, the direct ionization of protons is not a cause of upsets. This is because the deposited charge, which may initiate an upset, is proportional to the square of the atomic number of the ion. Therefore, proton-induced upsets are often caused by ionization of fragments and recoils, which are the reaction products (secondaries) of nuclear collisions of protons on silicon nuclei [2]. For an upset to occur, the generated charge must be collected at sensitive node in the microcircuit [3]–[7]. For the purpose of SEE investigation, the collected charge may originate from direct ionization of heavy ions, ionization of reaction products initiated by protons (or neutrons), a local charge enhancement, or elsewhere. However, there is one commonality: the charge collected at a sensitive region must be larger than the critical charge,  $Q_C$ , for the upset to occur.

For irradiation with ions, the probability of upset is normally expressed with a cross section, which is effectively the area of the sensitive region. Heavy-ion induced cross sections  $\sigma_{\text{ion}}$  are usually plotted in terms of the linear energy transfer (LET) of the incident ions. On the other hand, a proton-induced upset cross-section curve  $\sigma_p$  is normally plotted in terms of the energy

of protons. Therefore, a heavy-ion induced cross-section curve may not be directly compared to a proton-induced sensitivity curve for the same device. However, attempts have been made to transform a heavy ion sensitivity curve to a proton sensitivity curve in recent years.

Since energetic protons may produce nuclear fragments (secondaries) near an SEE sensitive region, some secondaries may cause upsets. The LET distribution of these secondaries has a nonlinear spread and it is dependent on the energy of incident protons. If we can establish a distribution function of “the number of secondaries versus LET of secondaries” for proton irradiation at a sensitive region, it may be possible to transform a “ $\sigma_{\text{ion}}$  versus LET (of ions) curve” to a “ $\sigma_p$  versus energy (of protons) curve.” However, we normally do not know the distribution of the secondaries and fragments in relationship to the location and the shape of sensitive nodes in a microcircuit. By making various assumptions and developing upset mechanisms from physics fundamentals, the effects of protons on microcircuits have been formulated. As a result, there are transformation equations and empirical rules with which one can derive the proton-induced single event effects (SEE) sensitivity of a microcircuit from an experimentally obtained heavy-ion induced SEE sensitivity [8]–[18]. In order to further investigate the relationship, we have measured the proton-induced and heavy-ion induced upset sensitivities using the Virtex-II FPGA. The technologies incorporated in this device type may not be the same as those studied earlier [19]. We compare the sensitivities using an equation derived for the PROFIT model [12] as an aid. Petersen’s model [13] as well as Edmonds’ model [16], [17] have also been used. These models are chosen because they have been utilized by the radiation effects community on various occasions.

## II. EXPERIMENTAL PROCEDURE

### A. Test Device

The device chosen for the current study is the Virtex-II X-2V1000. The device was procured in a 256-pin wire-bond standard ball gate array (BGA) package. It was fabricated using the “QPro radiation evaluation sample mask set” for the XQR2V1000 but unlike the XQR-type device, it was produced on bulk CMOS wafers (that is, without an epitaxial layer.) The mask is identical to one intended for the XQR (or Xilinx QPro) line of radiation hardened Virtex devices. The absence of the epitaxial layer is not expected to strongly affect upset cross sections in comparison to those obtained from ones with an epitaxial layer. The epitaxial layer in the XQR-type is intended to eliminate single event latchup (SEL) at very high LET

Manuscript received September 12, 2003; revised December 10, 2003.

R. Koga and J. George are with The Aerospace Corporation, El Segundo, CA 90245 USA (e-mail: rocky.koga@aero.org).

G. Swift, C. Yui, and L. Edmonds are with the Jet Propulsion Laboratory, Pasadena, CA 91109 USA (e-mail: gary.swift@jpl.nasa.gov).

C. Carmichael is with Xilinx, San Jose, CA USA (e-mail: carlc@xilinx.com).

T. Langley and P. Murray are with SEAKR Engineering, Centennial, CO 80111 USA (e-mail: tlangley@seakr.com).

K. Lanes and M. Napier are with Sandia National Laboratory, Albuquerque, NM 87123 USA (e-mail: krlanes@sandia.gov).

Digital Object Identifier 10.1109/TNS.2004.835057

values. The Virtex-II X-2V1000 was fabricated on a 0.15  $\mu\text{m}$  CMOS 8-layer metal process and included 40 block RAM's (737 280 bits), 432 maximum I/Os, and 2.8 M configuration bits [20]. These devices were obtained for the sole purpose of SEU testing. The X-2V1000 was ideal for SEU characterization because it was one member of the Virtex-II family that had a face-up die, suitable for heavy ion penetration. Prior to testing, the device was chemically etched to expose the die.

### B. Test Setup

The present SEU characterization of the Virtex-II FPGA is made possible with data collected from various static tests. Here "static" implies that the test circuit was not clocked during irradiation. Note that the total cross section in a space environment is expected to have some dynamic susceptibility that would add to the static susceptibilities reported here. The purpose of these tests was to determine the number of upsets in the configuration, block RAM and other internal components [20]. The test board was a HW-AFXBG256-200 prototype board connected to a host PC running custom test software via the Xilinx MultiLinx or JTAG cables. The test captured static configuration and block RAM data from the DUT (device under test) through a "service FPGA" on the prototype board. A specifically designed C++ based application named FIVIT (Fault Injection and Verification Tool) test software was used to configure the DUT and to read back SEUs in the memory cells. The features of FIVIT include the ability to set all user flip-flops to either "1s" or "0s" and capture their data, as well as to read and write to configuration registers such as the command register (CMD), frame length register (FLR), configuration option register (COR), control register (CTL), masking register for CTL (MASK), frame address register (FAR), CRC register, and the status register (STAT). Another useful utility added to FIVIT was the option of reading and writing to configuration registers through either the MultiLinx (SelectMAP port) mode or through the JTAG cable. This allowed us to use the speed of the SelectMap port while retaining the ability to recover SEU data via the JTAG port in the event of a SelectMap error. The capacity of the shift register used was  $(320 \times 32)$  9920 flip-flops for the present test samples. An HP6629A digital power supply was used to provide 3.3 V to the board and 1.5 V to the FPGA.

### C. Test Procedure

With each static test we observed and counted upsets for one or more of the following elements: configuration memory, block RAM and user flip-flops and latches. In addition to upsets in these elements, a number of single event functional interrupts (SEFI) were noted [21]. Charged particles altering the logic gates of the power-on-reset (POR) circuitry and SelectMap port were two of the more frequently occurring SEFIs, either resetting the device (resulting in a very low bias current condition) or disabling the communication between the DUT and FIVIT software, respectively [1]. A SelectMap SEFI as defined here is any functional problem that keeps us from getting perfect data retrieval while using the SelectMap port to communicate with the DUT, regardless of actual circuitry affected. We define a similar SEFI category for functional errors while using the JTAG port called the JCFG SEFI. The two categories clearly have some

TABLE I  
WEIBULL PARAMETERS FOR FOUR SETS OF HEAVY ION RESULTS

Section	Onset	Power	Width	Limit
Config	1	0.8	33	4.37E-8
BRAM	1	0.9	17	4.19E-8
POR	1.5	1.2	22	2.5E-6
SMAP	1.5	1	17	1.72E-6

overlap as they include SEFI types that affect areas of the chip unrelated to either of the actual communication port circuitry.

The cross section  $\sigma$  is calculated using the equation

$$\sigma = (N/F) s\theta$$

where N is the number of errors (counting all upset bits), F is the beam fluence in particles/cm<sup>2</sup>, and  $\theta$  is the angle between the beam and the chip-surface normal. The Virtex-II samples were tested without heating or cooling.

### D. Test Facilities

Testing was carried out at the Texas A&M University Texas A&M University Cyclotron, the Lawrence Berkeley National Laboratory 88-inch cyclotron facility, the Indiana University Cyclotron Facility, and the UC Davis Crocker Nuclear Laboratory. Devices were tested using heavy ions with an LET range of 1.5 to 63 MeV/(mg/cm<sup>2</sup>) and protons with energies from 3.8 to 200 MeV.

## III. HEAVY ION TEST RESULTS

Heavy ion test results are presented as combined cross-section curves for several sensitive sections of test samples. Weibull fit curves to the data and the fit parameters are given in Table I. In addition, we have shown an exponential curve to fit the data in the figure. The equation used to fit the data is

$$\sigma = \sigma_{\text{sat}} \exp(-L_{1/e}/\text{LET})$$

where  $\sigma_{\text{sat}}$  (a fitting parameter) is the saturation cross section and  $L_{1/e}$  (another fitting parameter) is the LET at which the cross section is  $1/e$  times the saturation cross section. To add a measure of conservatism, the fits for all the following curves have been adjusted upwards slightly to enclose as many data points as possible. These curves will be used to calculate associated proton cross sections (see Section IV.) The Xilinx Virtex-II FPGA type appears to have a higher SEE sensitivity when comparing to other FPGAs including Xilinx Virtex FPGAs [22].

### A. Configuration Memory

The configuration memory section is made up of many (2 787 740) bits. SEU cross sections of the configuration memory are shown in Fig. 1. The cross-section curve rises from a low LET value of about 2 MeV/(mg/cm<sup>2</sup>) and the curve appears to have reached the "saturated value" when the LET reaches about 60 MeV/(mg/cm<sup>2</sup>). The knee is rather round (not very sharp) and located at an LET value near 10 MeV/(mg/cm<sup>2</sup>). Fit parameters for the Weibull fit shown in the figure are given in Table I.

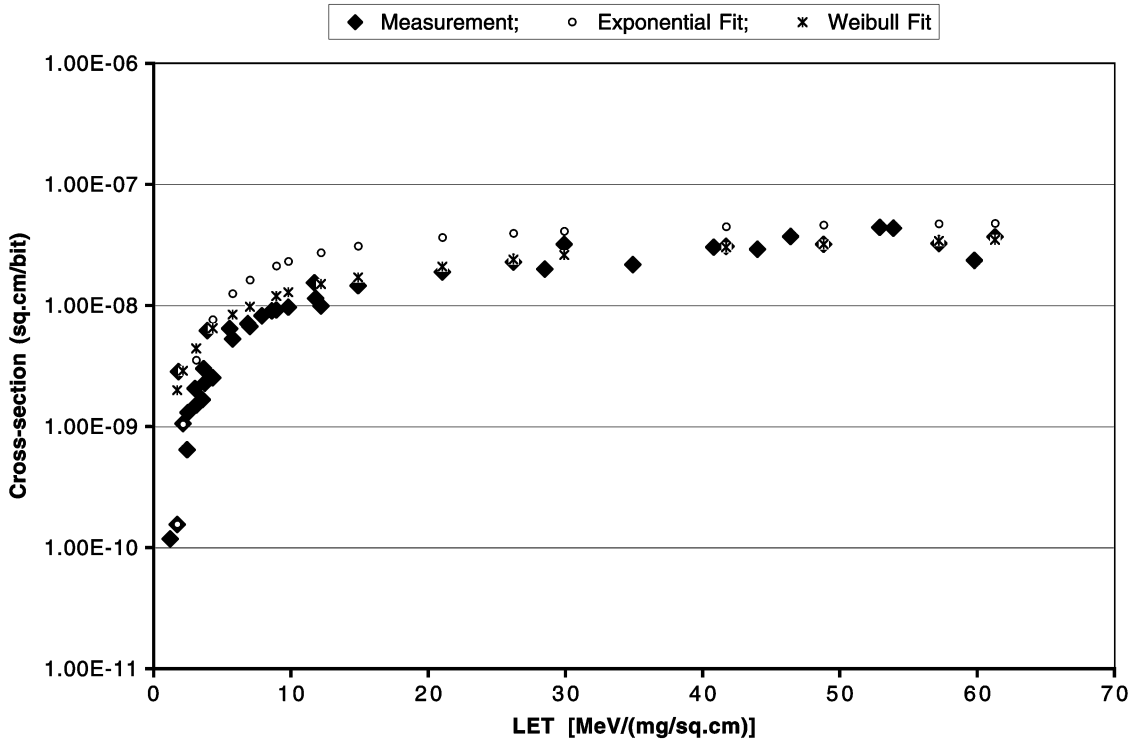


Fig. 1. Heavy-ion induced SEUs for configuration memory.

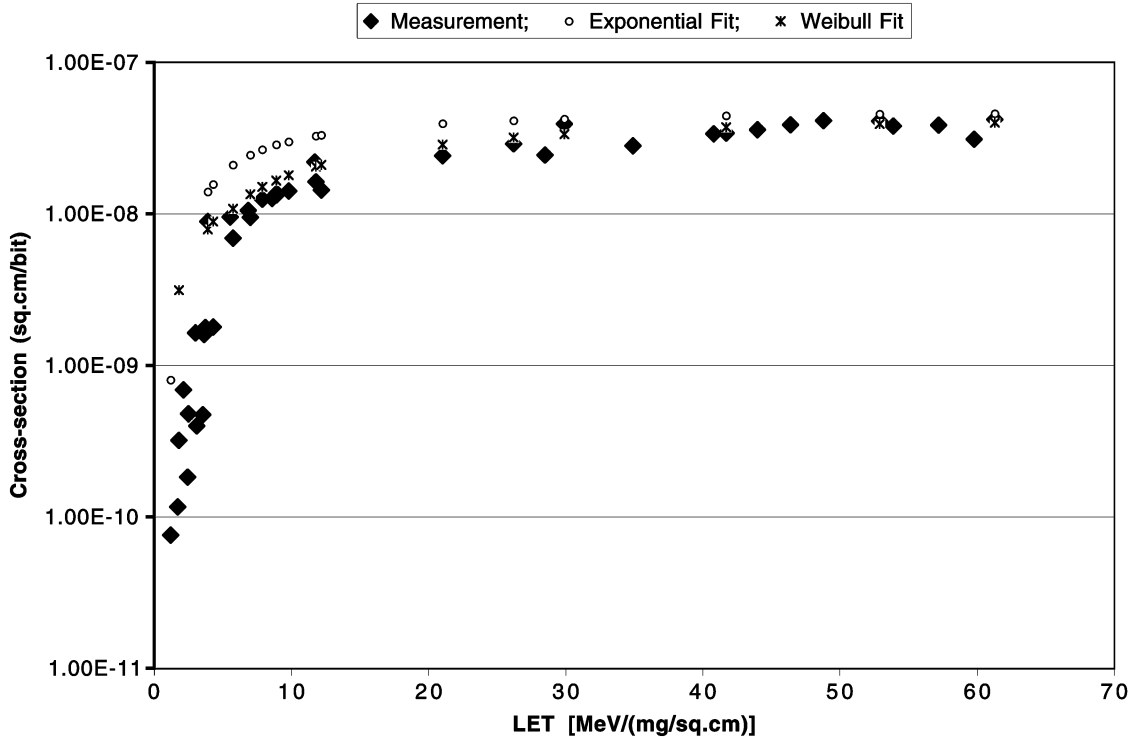


Fig. 2. Heavy-ion induced SEUs for Block RAM.

*B. Block RAM*

The block RAM section is made up of 737 280 bits. The SEU cross sections of the block RAM are shown in Fig. 2. The cross-section curve appears to rise sharply (as compared to that for the configuration memory upset curve) starting from an LET value

of about 2 MeV/(mg/cm<sup>2</sup>). Fit parameters for the Weibull fit shown in the figure are given in Table I.

*C. Power-on-Reset (POR) Circuit*

There is a section in the test device that serves to reset the device during a power on [20]. Under normal operating con-

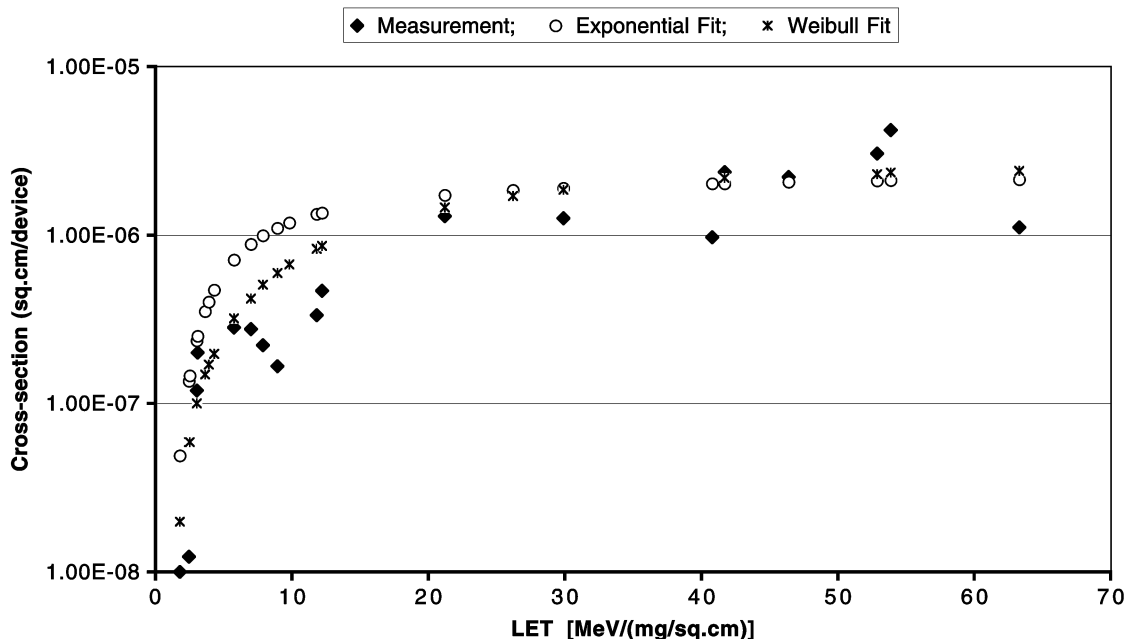


Fig. 3. Heavy-ion induced POR SEFI.

ditions, this section would not be activated until the power has been turned-off and then turned-on. However, a heavy-ion induced upset in the power-on-reset section may cause an unexpected reset of the test device and the bias current would drop. These are SEFI events, and were observed during irradiation. The POR SEFI cross-section curve has been plotted in Fig. 3. The measured curve has a relatively sharp rise starting from an LET value near 3 MeV/(mg/cm<sup>2</sup>). The plotted points in the cross-section curve are based on only a few observed SEFIs each, especially at low LET values. This may be the reason that the curve is not smooth. Since we do not know exactly the number of bits involved in this type of upset, the vertical axis for the plot is “cross section (cm<sup>2</sup>/device).” Fit parameters for the Weibull curve shown in the figure are given in Table I.

#### D. SelectMap and JTAG Port Circuits

A test sample (DUT) may be interfaced via the SelectMap or JTAG communication ports. Under normal operations all data from the sample are received without an error. An upset in the relevant circuit may bring about errors in received data. A SelectMap or JTAG (JTAG) SEFI is an upset that keeps us from getting perfect data from the DUT while using the respective port. These types of SEFIs encompass some other SEFIs, which may not be directly related to the port circuitry. An example is the FAR SEFI, which specifically affects the frame address register (see Section II-B.) For simplicity, we grouped all SEFIs observed while using either port together. The SelectMap SEFI sensitivity is shown in Fig. 4. The cross sections have the units of (cm<sup>2</sup>/device.) As before, only a few errors contribute to each plotted point, especially at low LET values. This may be the reason the curve is not smooth. Fitted curves for both the Weibull and exponential formulations are shown in the figure. The parameters of the Weibull curve are given in Table I.

#### E. Single Event Latchup

Single event latchup (SEL) is a potentially destructive high current state induced by the passage of a charged particle. The present test samples did not show any sign of latchup. Therefore no latchup curves are presented.

### IV. MODELS SIMULATING PROTON SENSITIVITY

There are models with which one can estimate proton sensitivity without testing the pertinent microcircuit with protons. Inputs for these models include heavy ion test results. We have chosen three models. One, the Edmonds model, provides an upper bound of proton sensitivity cross section while the others show proton cross-section curves.

#### A. Edmonds' Model

A model by Edmonds uses a generic charge collection efficiency function to relate heavy ion to proton cross sections [16], [17]. The most practical result is an upper bound for proton SEE cross sections. To calculate the upper bound, the associated heavy ion cross-section curve may be integrated along LET values. We have shown such curves, exponential fit curves, in our heavy ion test results (see Figs. 1–4).

#### B. PROFIT Model

This model enables us to calculate a proton-induced cross-section curve of a microcircuit from a sensitivity curve obtained with heavy ions [12]. Heavy ion sensitivity results as a function of LET are fitted by a Weibull curve with associated parameters. In the PROFIT model, LET is transposed to the energy of the recoil heavy ion. Under elastic scattering the energy of the recoil may then be expressed in terms of the primary proton energy. All these conversions are made in the formulation of the PROFIT model. The result is an equation describing a proton-induced SEE cross-section curve expressed in terms of proton energy.

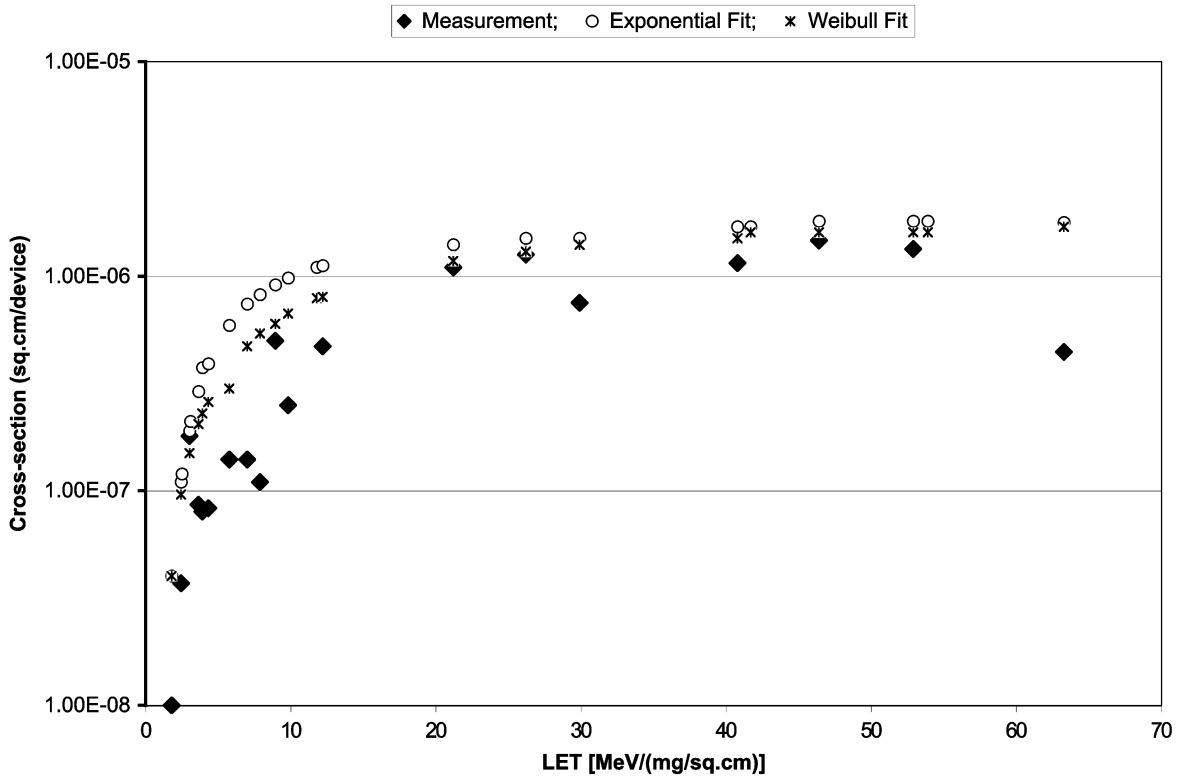


Fig. 4. Heavy-ion induced SelectMap SEFI.

### C. Petersen's Model

A model by Petersen enables us to predict an upset rate in space for some microcircuits if we have associated heavy ion-induced sensitivity curves [13]. The heavy ion sensitivity of a microcircuit is converted to the threshold energy  $A$  for proton interaction by an equation,  $A = L_{0,1} + 15$ . Here  $L_{0,1}$  is the LET level at which the cross section is reduced to 10% of the saturation cross-section value as defined in [13]. The scaled quantity  $A$  is the Bendel  $A$  parameter in the one parameter model used to predict proton sensitivity [1]. The task of obtaining  $L_{0,1}$  is aided by a Weibull fit curve for heavy ion data. Then, we can calculate relevant proton upset cross sections derived under Bendel's one parameter model.

## V. MEASURED AND PREDICTED PROTON-INDUCED UPSETS

We have experimentally obtained proton-induced SEE sensitivities of test samples. They are compared to those predicted from the PROFIT simulation model and the Bendel one-parameter model utilized by Petersen. The upper bounds predicted with the use of Edmonds' model are also shown.

### A. Proton-Induced SEU Sensitivity for Configuration Memory

The proton SEU sensitivity for the configuration memory is shown in Fig. 5. The measured values reach a plateau at about 10 MeV. The cross sections at higher energy levels have very similar values. The SEU cross section at the proton energy of 3.8 MeV is about  $1 \times 10^{-14}$  cm<sup>2</sup>/bit. Since we have not used protons with lower energies than 3.8 MeV, this data point shows the smallest cross-section value. The prediction with the use of the Bendel one parameter equation (Petersen's model) shows larger cross sections at higher energy values. The upper bound

predicted with the use of Edmonds' model appears to show a good agreement with measured results. The PROFIT curve lies below the measured values, however, the shape of the curve resembles the measured results.

### B. Proton-Induced SEU Sensitivity for Block RAM

The proton SEU sensitivity for the Block RAM is shown in Fig. 6. The measured values reach a plateau at about 10 MeV. The cross sections at higher energy levels have very similar values. The SEU cross section at the proton energy of 3.8 MeV is just below  $1 \times 10^{-14}$  cm<sup>2</sup>/bit. Since we have not used protons with lower energies than 3.8 MeV, this data point shows the smallest cross-section value. The prediction from Bendel's one parameter equation (Petersen's model) also gives larger cross sections at higher energies. This curve rises slightly higher than the one for configuration memory. The upper bound predicted with Edmonds' model shows very good agreement with the measured data. The PROFIT curve lies below the measured values but again, the shape of the curve resembles the data.

### C. Proton-Induced POR SEFI

The proton-induced POR SEFI sensitivity is shown in Fig. 7. The SEFI cross section at the proton energy of 6.8 MeV (the lowest energy) is an upper limit, since we did not detect any SEFIs at this energy. All other cross sections are above  $1 \times 10^{-13}$  cm<sup>2</sup>/device. No more than a few errors contribute to each measured point, leading to large statistical uncertainties. The prediction with Petersen's model gives larger cross sections at proton energies beyond 50 MeV. Edmonds' upper bound is higher than the measured value. The PROFIT curve matches measured values above 25 MeV.

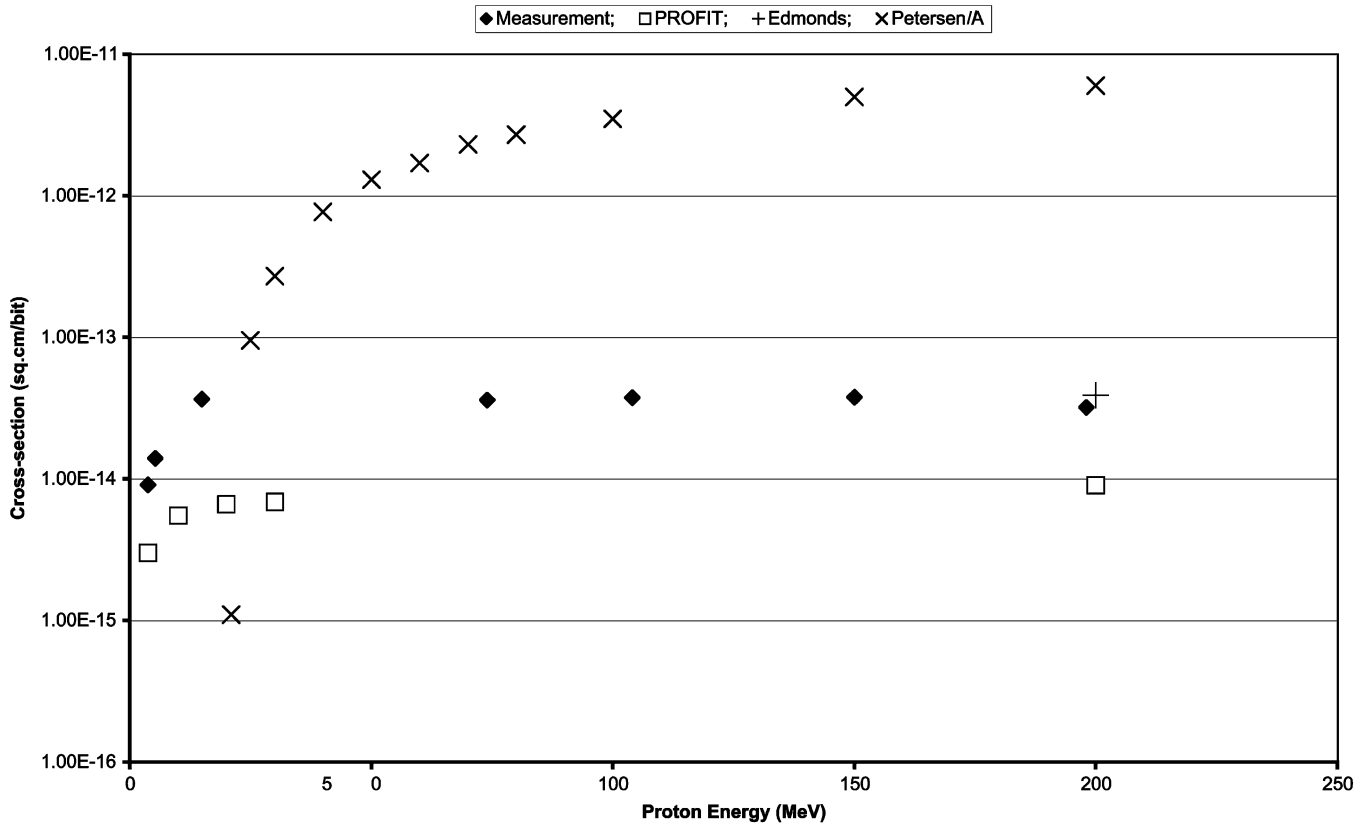


Fig. 5. Proton-induced SEU sensitivity for configuration memory.

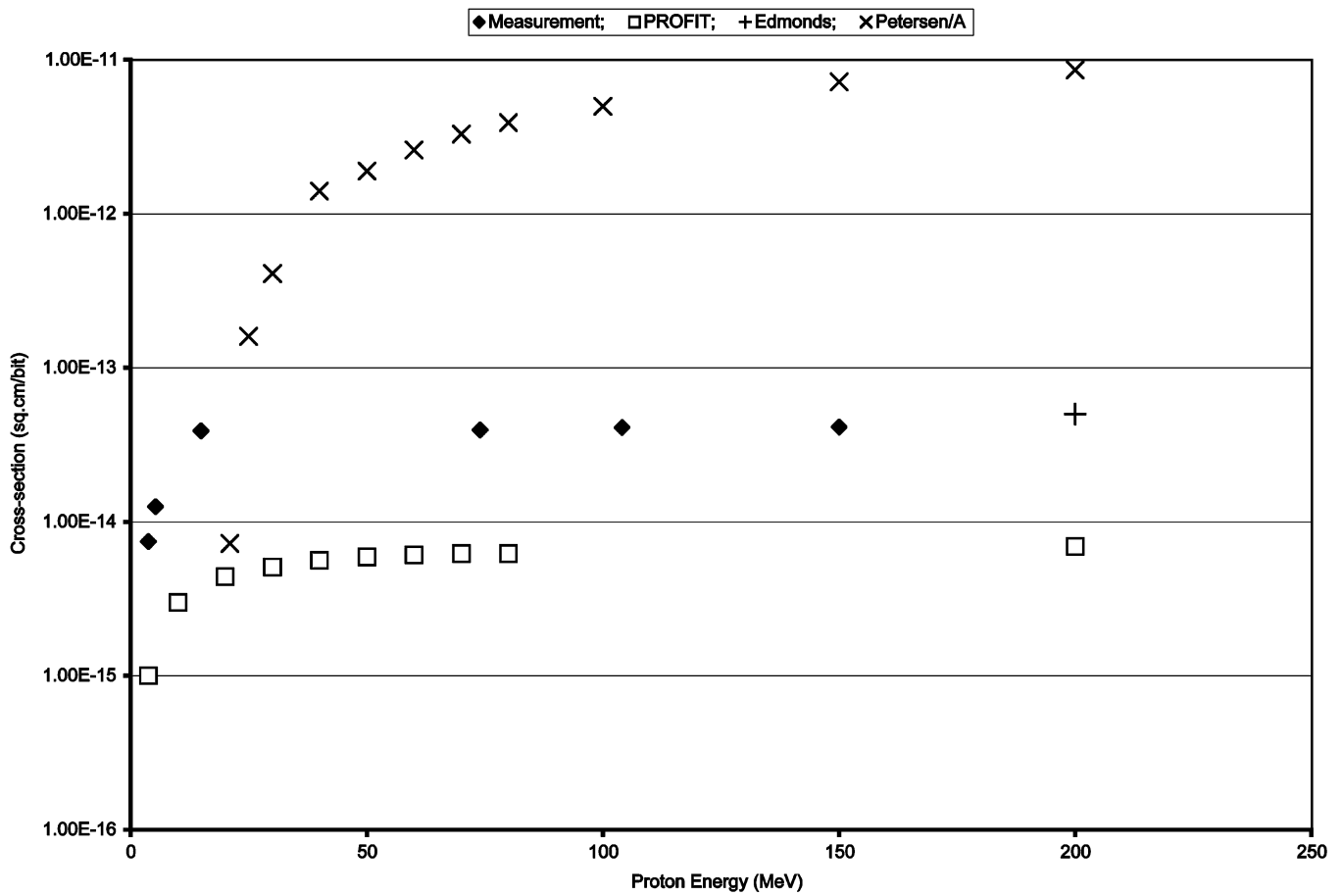


Fig. 6. Proton-induced SEU sensitivity for Block RAM.

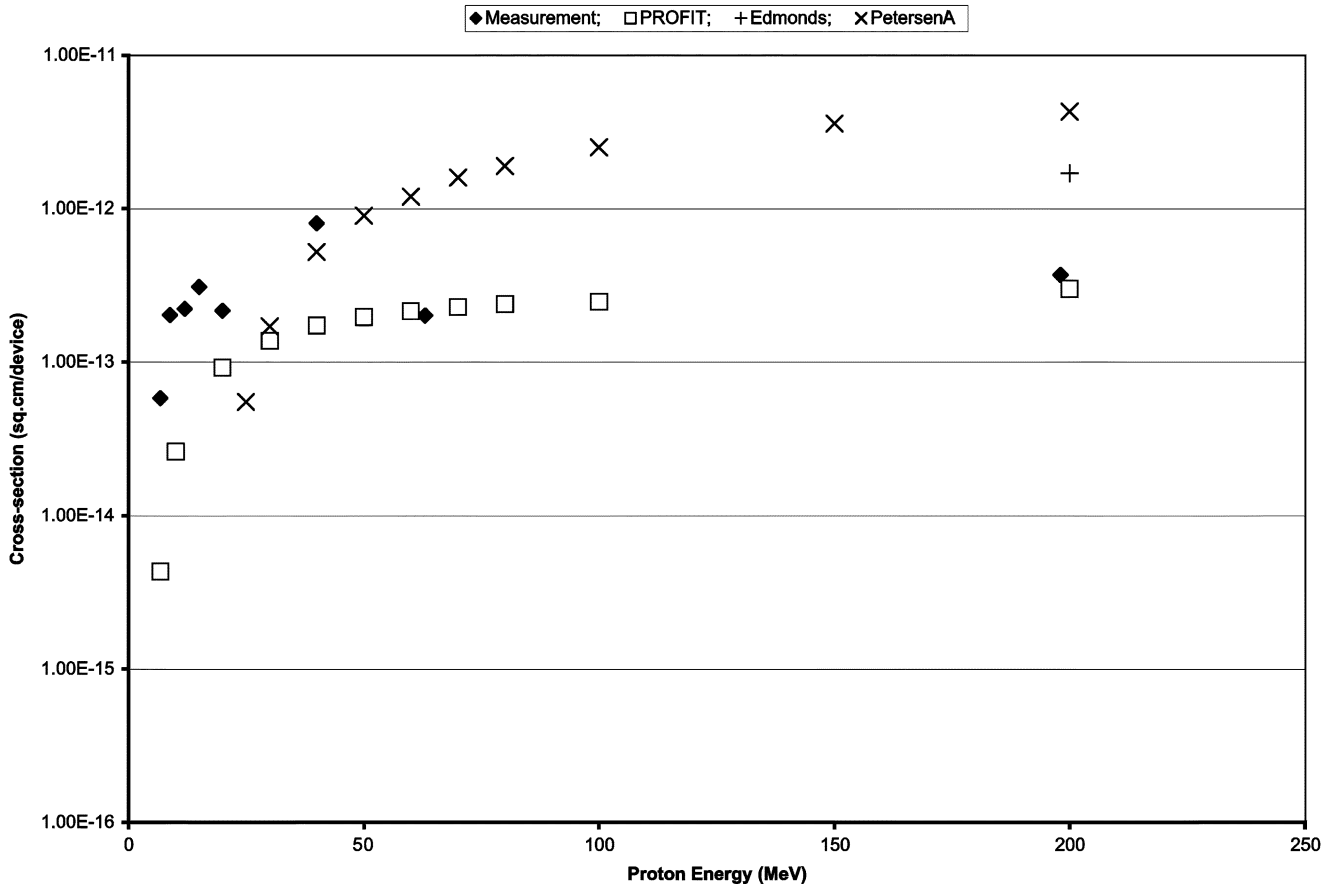


Fig. 7. Sensitivity to proton-induced POR SEFI.

#### D. Proton-Induced SelectMap SEFI

The proton-induced SelectMap SEFI sensitivity is shown in Fig. 8. The SEFI cross section at the proton energy of 6.8 MeV (the lowest energy) is just above  $1 \times 10^{-13} \text{ cm}^2/\text{device}$ . All cross sections at energy values beyond 30 MeV are higher than those at lower energy values. The number of errors involved in calculating the cross sections is no more than a few for SelectMap SEFIs. This may be the reason that the curve is not smooth. The prediction with the use of the Bendel one parameter equation (Petersen's model) results in larger cross sections at energy values beyond 30 MeV. The upper bound predicted with the use of Edmonds' model appears to show very good agreement with measured results. The PROFIT curve lies slightly below the measured values.

#### E. Proton-Induced JCFG SEFI

Proton-induced JCFG SEFI sensitivity is shown in Fig. 9. As with the other SEFIs, the number of errors contributing to each point is small. This probably contributes to the shape of the curve. Despite the low statistical significance, these results appear to resemble those for SelectMap SEFI. Predictions based on the heavy ion JCFG measured data were not yet available as of this writing.

## VI. DISCUSSIONS

Models that predict proton-induced sensitivities often use associated heavy ion induced sensitivities as input. Therefore a

higher heavy-ion induced sensitivity would, in general, predict a higher proton-induced sensitivity. This proportionality is embedded in the PROFIT model as well as in many other prediction models. However, this proportionality seems not to yield the best fit when we compare the configuration memory and Block RAM sensitivities with PROFIT. The predicted values are substantially lower than measured values. Yet, among various single event effects, there are some phenomena, such as POR SEFI sensitivities, for which it is possible to make a reasonably accurate prediction of the proton-induced cross-section curve with the knowledge of the associated heavy-ion induced cross section curve. The above examples of agreement and disagreement show that the PROFIT model does not consistently show good agreements for the present test samples. However, the shape of the proton cross section curve as derived by the PROFIT model seems to resemble the actually measured curve. Therefore, we may be able to use protons at one high energy level, e.g., 200 MeV, to obtain a measured cross section to scale the PROFIT curve.

The Petersen's model is very simple. However, it is based on relatively old proton interaction mechanisms for which proton induced SEE cross sections continuously increase with its energy. This trend does not seem to hold in the new submicron devices such as the Virtex-II FPGA. Proton SEE test results of submicron devices have shown relatively flat cross sections at higher energy values. Since the nuclear interactions of protons with silicon atoms tend to increase with higher energies [23], this may be another indication that proton-induced SEEs are

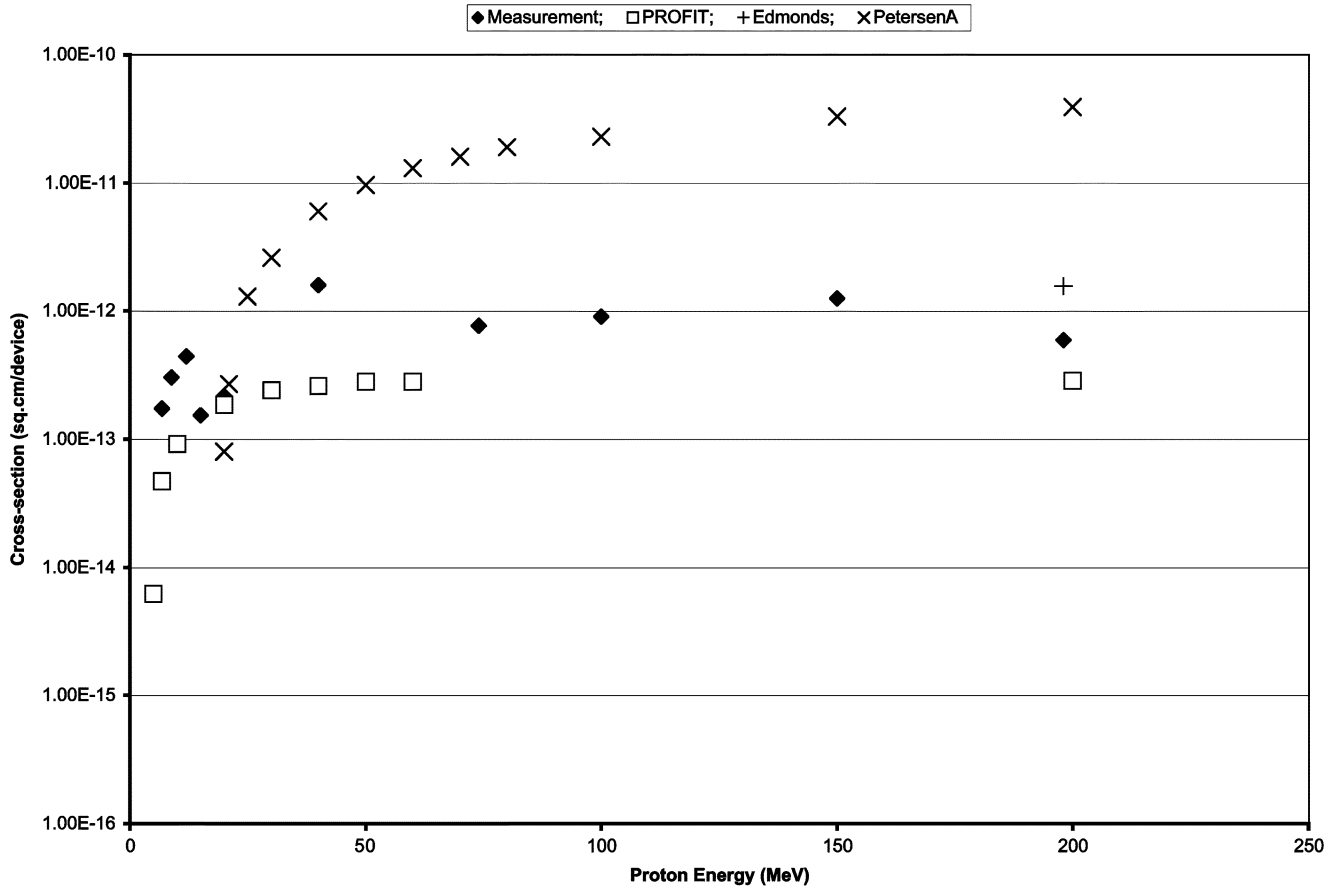


Fig. 8. Sensitivity to proton-induced SelectMap SEFI.

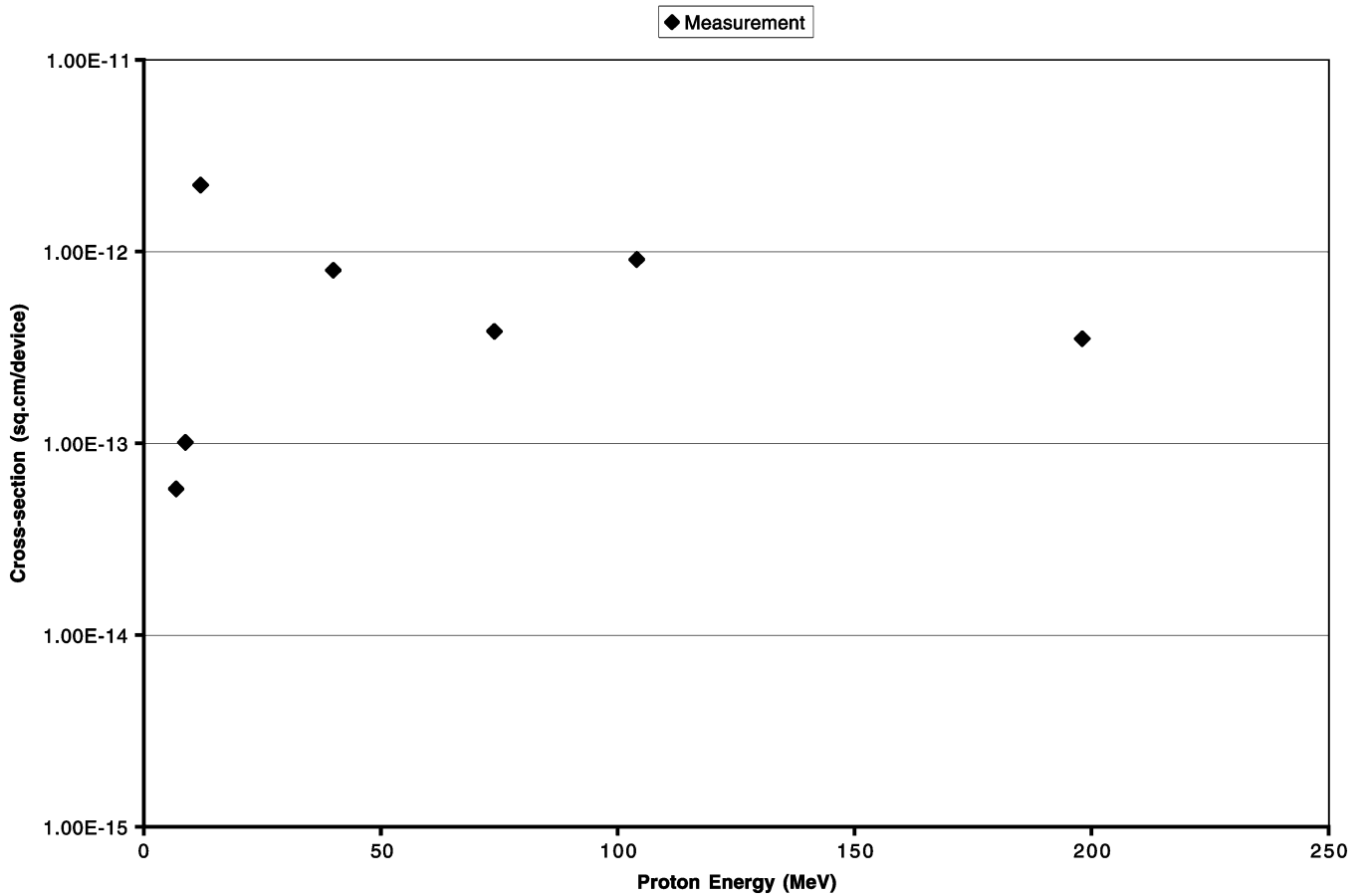


Fig. 9. Sensitivity to proton-induced JCFG SEFI.

affected by various factors including the energy distributions of the secondaries. Other factors may include the physical distribution of insulators such as buried oxides in silicon [24] and the complicated geometry of SEE sensitive regions [19]. These lead to considerations that the charge collected from a depletion region as an ion passes through it is only a part of the charge causing upsets in the region for modern microcircuits [25].

Practical results obtained with the use of Edmonds' model are upper bounds for proton SEE cross sections. They seem to show reasonably good agreement in all of the cases that we have considered.

The mechanism involved in proton-induced upsets may stem from both elastic and inelastic proton interactions. We have observed proton-induced upsets with present test samples at a 3.8 MeV proton energy (see Figs. 5 and 6). Since this does not appear to be the threshold energy level, upset sensitivities may be significant below 3.8 MeV. Also, the proton cross sections do not vary appreciably at these energy levels. Therefore, we think upsets are not caused by direct ionization of protons. The results suggest, rather, that elastic interactions contribute to upsets. Since the PROFIT model incorporates the elastic interaction in its formulation, its proton-induced cross sections at low energy levels seem to show a reasonably good agreement for some results (see Fig. 7). We think the elastic interaction is a major contributing factor at these energy levels.

We have observed multiple-bit upsets caused by one heavy ion strike in many microcircuits, while such events are rare when protons are used. Since the models that we have considered do not specifically include the effect of multiple-bit upsets, we have not obtained the numbers of multiple-bit upsets in our measurements. This lack of consideration of multiple-bit upsets may be a contributing factor in some discrepancies between the measured and PROFIT predicted values.

## VII. CONCLUSION

It appears that a comparison of proton-induced and heavy-ion induced sensitivities will not lead to the formulation of a simple relationship between them. Even though we have used only a few prediction models, we think that the complex nature of the undertaking is too great to be accommodated by a universally acceptable prediction model. Since both PROFIT and Petersen's models for Virtex-II show higher energy threshold values for proton-induced sensitivities than measured ones, we cannot use these models to obtain threshold values for the Xilinx Virtex-II devices. The energy threshold values for some SEUs appear to be below 3.8 MeV for the Virtex-II FPGA.

## ACKNOWLEDGMENT

The authors gratefully acknowledge the assistance of the on-site staffs at the Texas A&M University Cyclotron Institute, the Lawrence Berkeley National Laboratory 88" cyclotron, the Indiana University Cyclotron Facility, and the University of California (Davis) Crocker Nuclear Laboratory.

## REFERENCES

- [1] C. Yui, G. Swift, and C. Carmichael, "Single event upset susceptibility testing of the Xilinx Virtex-II FPGA," in *2002 MAPLD*, vol. IV, 2002.
- [2] W. L. Bendel and E. L. Petersen, "Proton upsets in orbit," *IEEE Trans. Nucl. Sci.*, vol. 30, pp. 4481–4485, 1983.
- [3] P. J. McNulty *et al.*, "Proton-induced nuclear reactions in silicon," *IEEE Trans. Nucl. Sci.*, vol. 28, pp. 4007–4012, 1981.
- [4] J. M. Bisgrove *et al.*, "Comparison of soft errors induced by heavy ions and protons," *IEEE Trans. Nucl. Sci.*, vol. 33, pp. 1571–1576, 1986.
- [5] R. Koga *et al.*, "SEU test techniques for 256 K SRAMs and comparison of upsets induced by heavy ions and protons," *IEEE Trans. Nucl. Sci.*, vol. 35, pp. 1638–1643, 1988.
- [6] T. Bion and J. Bourrieau, "A model for proton-induced SEU," *IEEE Trans. Nucl. Sci.*, vol. 36, pp. 2281–2286, 1989.
- [7] P. M. O'Neill *et al.*, "Internuclear cascade evaporation model for LET spectra of 200 MeV protons," *IEEE Trans. Nucl. Sci.*, vol. 45, pp. 2467–2474, 1998.
- [8] B. Doucin *et al.*, "Characterization of proton interactions in electronic components," *IEEE Trans. Nucl. Sci.*, vol. 41, pp. 593–600, 1994.
- [9] J. Barak *et al.*, "A simple model for calculating proton induced SEU," in *RADECS95*, 1995, pp. 431–436.
- [10] J. G. Rollins, "Estimation of proton upset rates from heavy ion test data," *IEEE Trans. Nucl. Sci.*, vol. 37, pp. 1961–1965, 1990.
- [11] C. Inguibert *et al.*, "Proton upset rate simulation by a Monte Carlo method," *IEEE Trans. Nucl. Sci.*, vol. 44, pp. 2243–2249, 1997.
- [12] P. Calvel *et al.*, "An empirical model for predicting proton induced upset," *IEEE Trans. Nucl. Sci.*, vol. 43, pp. 2827–2832, 1996.
- [13] E. L. Petersen, "The relationship of proton and heavy ion upset thresholds," *IEEE Trans. Nucl. Sci.*, vol. 39, pp. 1600–1604, 1992.
- [14] E. Normand, "Extensions of the burst generation rate method for wider application to proton/neutron-induced single event effects," *IEEE Trans. Nucl. Sci.*, vol. 45, pp. 2904–2914, 1998.
- [15] R. A. Reed *et al.*, "A simple algorithm for predicting proton SEU rates in space compared to the rates measured on the CRRES satellite," *IEEE Trans. Nucl. Sci.*, vol. 41, pp. 2389–2395, 1994.
- [16] L. D. Edmonds, "Proton SEU cross sections derived from heavy-ion test data," *IEEE Trans. Nucl. Sci.*, vol. 47, pp. 1713–1728, 2000.
- [17] L. D. Edmonds, "SEU cross sections derived from a diffusion analysis," *IEEE Trans. Nucl. Sci.*, vol. 43, pp. 3207–3217, Dec. 1996.
- [18] J. Barak, "Empirical modeling of proton induced SEU rates," in *RADECS99*, 2000, pp. 167–172.
- [19] R. Koga *et al.*, "Comparison of heavy ion and proton induced single event effects (SEE) sensitivities," *IEEE Trans. Nucl. Sci.*, vol. 49, pp. 3135–3141, 2002.
- [20] Virtex-II Platform Handbook. Xilinx. [Online]. Available: <http://www.xilinx.com/products/virtex/handbook/index.htm>
- [21] R. Koga *et al.*, "SEFI sensitivity in microcircuits," in *RADECS97*, 1997, pp. 311–318.
- [22] C. Carmichael *et al.*, "Proton testing of SEU mitigation methods for the Virtex FPGA," in *2001 MAPLD*, vol. III, 2001, pp. 23–25.
- [23] P. J. McNulty *et al.*, "Upset phenomena induced by energetic protons and electrons," *IEEE Trans. Nucl. Sci.*, vol. 27, pp. 1516–1522, 1980.
- [24] V. Ferlet Cavois *et al.*, "Charge collection by capacitance influence through isolation oxides," *IEEE Trans. Nucl. Sci.*, vol. 50, 2003.
- [25] R. Koga *et al.*, "Serendipitous SEU hardening of resistive load SRAMs," in *RADECS95*, 1995, pp. 354–358.